Heliyon 11 (2025) e42159

Contents lists available at ScienceDirect

Heliyon

journal homepage: www.cell.com/heliyon

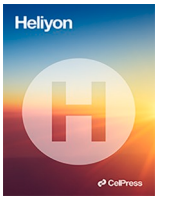

Research article

Caesalpinia sappan L. ethyl acetate extract regulated angiogenesis in atherosclerosis by modulating the miR-126/VEGF signalling pathway

Yue He [a,1], Chao Huang [a,*], Jingjing Chen [b], Weizeng Shen [a]

[a] *Department of Traditional Chinese Medicine, The Second Affiliated Hospital of Shenzhen University, People's Hospital of Shenzhen Baoan District, Shenzhen, 518000, Guangdong, China*
[b] *Changchun University of Traditional Chinese Medicine, Changchun, 130000, Jilin, China*

ARTICLE INFO

Keywords:
Caesalpinia sappan L.
Atherosclerosis
Angiogenesis
miR-126/VEGF

ABSTRACT

Aims of the study: To investigate the regulatory mechanism of *Caesalpinia sappan* L. ethyl acetate extract (CSEAE) on angiogenesis in atherosclerosis (AS) based on the miR-126/VEGF signalling pathway.

Materials and methods: Our study first screened for differentially expressed microRNAs (miRNAs) associated with AS using the Gene Expression Omnibus (GEO) public database at the National Center for Biotechnology Information (NCBI) and R language software. Subsequently, our study verified the target-regulatory relationship between miR-126 and vascular endothelial growth factor (VEGF) in human umbilical vein endothelial cells (HUVECs) by using the "TargetScan" website and dual-luciferase reporter assay. In cellular experiments, Our study used cell proliferation assays and flow cytometry to assess the effects of CSEAE-Mediated serum on the proliferation and apoptosis of HUVECs. In animal experiments, our study used HE staining, Oil Red O staining and immunohistochemistry (IHC) staining to detect plaque area/lumen area (%), lipid area/plaque area (%) and microvessel density (MVD) in mouse aortas. In addition, our study performed RT−PCR, ELISA and Western blot assays in ex vivo and in vivo experiments.

Results: A total of 39 differentially expressed miRNAs of AS were identified, among which the miR-126 expression level was significantly downregulated. Dual luciferase reporter gene assay results showed that miR-126 and VEGF have a targeting relationship, and the miR-126 mimic could inhibit the luciferase activity of the wild-type VEGF reporter gene vector (p value < 0.01). In cellular experiments, cell proliferation assays and flow cytometry results showed that CSEAE-Mediated serum significantly increased the proliferative activity after 24–72 h of treatment (p-value <0.01) and decreased the apoptotic level of HUVECs (p value < 0.01), and RT−PCR results showed that CSEAE-Mediated serum significantly upregulated the expression of miR-126 (p value < 0.01) and downregulated the expression of VEGF mRNA in HUVECs (p value < 0.01). In vivo experiments, HE staining and IHC staining showed that CSEAE significantly reduced the MVD in the aorta and plaques of mice (p value < 0.01) and significantly reduced the aortic plaque area/lumen area (%) (p value < 0.01). Moreover, RT−PCR assay and Western blot analysis results showed that CSEAE significantly upregulated the expression of miR-126 (p value < 0.01), downregulated the expression of VEGF mRNA (p value < 0.01), and decreased the protein

* Corresponding author.
E-mail address: huangchao06@163.com (C. Huang).
[1] Contributing authors: 2865209579@qq.com

https://doi.org/10.1016/j.heliyon.2025.e42159
Received 12 June 2024; Received in revised form 20 January 2025; Accepted 20 January 2025
Available online 22 January 2025

expression levels of VEGF (p value < 0.01), phosphatidyl-inositol-3-kinase (PI3K) (p value < 0.01), and Ser/Thr-protein kinase (AKT1) (p value < 0.01) in mouse aortas, while ELISA showed that CSEAE significantly reduced the serum levels of vascular endothelial growth factor receptor (VEGFR2) (p value < 0.01) and hypoxia-inducible factor-1 (HIF-1) (p value < 0.01) in mice.
Conclusion: This study emphasises CSEAE as a natural medicinal extract for the treatment of AS that can improve the migratory viability and reduce the apoptosis of HUVECs to maintain the health of the arterial endothelial microenvironment, while CSEAE also inhibits angiogenesis and delays plaque formation in ApoE−/− mice, suggesting that the therapeutic effect of CSEAE for AS may be related to its inhibition of neovascularisation and that its molecular mechanism may be related to the miR-126/VEGF signalling pathway.

Abbreviations

Abbreviations	Full names
CSEAE	*Caesalpinia sappan* L. Ethyl Acetate Extract
AS	Atherosclerosis
miRNAs	microRNAs
GEO	Gene Expression Omnibus
NCBI	National Center for Biotechnology Information
ECs	Endothelial Cells
HUVECs	Human Umbilical Vein Endothelial Cells
Ox-LDL	Oxidized-Low-Density Lipoprotein Cholesterol
VEGF	Vascular Endothelial Growth Factor
IHC	Immunohistochemical
MVD	Microvessel Density
VEGFR2	Vascular Endothelial Growth Factor Receptor 2
HIF-1	Hypoxia Inducible Factor-1
CVDs	Cardiovascular diseases
TCM	Traditional Chinese medicine
CMC	Carboxymethyl Cellulose
PBS	Phosphate Buffered Saline
SD	Sprague-Dawley

1. Introduction

Cardiovascular diseases (CVDs) are the leading cause of death globally, while atherosclerosis (AS) is one of the most common pathological underpinnings of CVDs. Approximately 17.9 million people die annually from CVDs, with more than four-fifths of these deaths due to myocardial infarction and stroke, both of which, notably, are typically AS-related cardiovascular diseases [1]. There are risk factors associated with AS, including genetic factors, age and sex, smoking, physical activity and dietary habits, body mass index, cholesterol levels, blood pressure levels, blood sugar levels, and bacterial and viral infections, according to the American Heart Association (http://www.heart.org). Angiogenesis is one of the important mechanisms of endothelial microenvironment remodelling and plaque formation [2]. Currently, a variety of drugs can target the above single or multiple mechanisms to play a therapeutic role in the treatment of AS, such as statin drugs, which are currently the most widely used oral drugs. However, taking Western medicine to treat AS also has a large residual risk. Studies have found that Traditional Chinese medicine (TCM) has obvious advantages in preventing and treating AS, which can effectively alleviate disease progression at a low price and reduce the development of drug resistance and hepato-renal toxicity [3].

Caesalpinia sappan L., whose full botanical plant name is *Biancaea sappan* (L.) Tod. (www.worldfloraonline.org.), and scientific name of common or pharmaceutical names was retrieved on MPNS (http://mpns.kew.org) as or *Caesalpinia sappan* L. As an ancient Chinese herb, *Caesalpinia sappan* L. is mainly found in the provinces of Guangdong, Guangxi, Yunnan, Sichuan, and Taiwan, and the herbal medicine comes from the dried heartwood of *Caesalpinia sappan* L. The ethnopharmacological applications of *Caesalpinia sappan* L. have been documented in ancient Chinese literature, such as “Xin xiu Ben Cao” and “Ben Cao Jing Shu”, and were formally included in the “Pharmacopoeia of the People’s Republic of China” in 2020. *Caesalpinia sappan* L. is a natural plant-derived drug widely used in traditional Chinese medicine for the treatment of cardiovascular diseases. In ancient times, *Caesalpinia sappan* L. was mainly used by TCM for the treatment of bruises, broken bones, tendon injuries, blood stasis, swelling pains, stabbing pains in the chest and abdomen, carbuncles, gangrene, menstrual closure, dysmenorrhoea, and postpartum stasis. Modern medical studies have found that *Caesalpinia sappan* L. ethyl acetate extract (CSEAE), an effective extract of *Caesalpinia sappan* L., has antioxidant, anti-inflammatory and anticancer effects [4,5]. Further pharmacological studies have revealed that CSEAE contains a variety of bioactive compounds, including brazilin, papaya chalcone and protopapain A. These compounds have been shown to reduce inflammation, resist immune stimulation, have antioxidant properties, enhance blood circulation and promote wound healing [6]. Currently, CSEAE has been used as a therapeutic agent for a range of diseases, such as atherosclerosis [7], acute liver injury [8], diabetes and its secondary complications [9] and respiratory diseases [10,11]. A large number of studies have elucidated the pharmacological effects of CSEAE, however, there is a lack of contemporary pharmacological studies on the regulation of angiogenesis in AS.

In recent years, *Caesalpinia sappan* L. extract has made many gratifying achievements in the study of cardiovascular diseases. Studies have found that the flavonoids in the extract have antioxidant effects [12,13], which can remove free radicals in the body and reduce oxidative stress, thereby protecting the cardiovascular system. Besides, the extract inhibits the release of inflammatory mediators [14], such as tumor necrosis factor α (TNF-α) and interleukin 6 (IL-6), which helps reduce inflammatory responses in cardiovascular disease. Some components of the extract can inhibit platelet aggregation and thrombin activity [15], prevent thrombosis, improve vascular endothelial function, promote vasodilation, reduce blood pressure and improve blood circulation [6]. Some components can protect the heart from ischemia-reperfusion injury and reduce myocardial infarction size [16]. Some studies have shown that the *sappan* extract is able to reduce blood cholesterol and triglyceride levels, which can help prevent atherosclerosis [17]. In addition, the S*appan* extract can also inhibit the development of atherosclerosis and reduce plaque formation [18].

Bioinformatics research methods are widely used in the field of discovering new disease targets and detection indicators, which predict differentially expressed genes in diseases by detecting and comparing genes in normal individuals and disease models. Recently, many advances have also been made in human genetics research for people with AS, such as DNA, mRNA, and noncoding RNAs (e.g., differentially expressed microRNAs (miRNAs) and long noncoding RNAs) [19]. In this study, bioinformatics analysis, in vitro experiments, and in vivo experimental studies were used to elucidate the biological basis and mechanisms of CSEAE in the treatment of AS. These efforts aimed at discovering the potential risk factors and therapeutic targets of AS, exploring the mechanism of the anti-AS effect of CSEAE, providing directions for the clinical research of CSEAE in the treatment of AS, and laying the theoretical foundation for its clinical application.

2. Material and methods

2.1. Bioinformatics analysis

2.1.1. Validation of miR-126 differential expression in the serum of AS patients

Differential analysis of miRNA expression levels in the serum of AS and non-AS patients was performed by using R software, annotating the downloaded platform file from the Gene Expression Omnibus (GEO) public database at the National Center for Biotechnology Information (NCBI) as a matrix file (GSE96621) [20], performing comparative matrix design using the Limma software package, and fitting a linear model for comparison. Tests were then performed using the Bayesian method to screen for significantly differentially expressed miRNAs in AS with "p value < 0.05, logFC ≥ 0.5 or logFC ≤ -0.5" to validate that the miR-126 gene was significantly differentially expressed in the serum of AS patients. Finally, cluster analysis heatmaps and volcano plots were drawn using an online mapping website (https://www.bioinformatics.com.cn) to visualise the results of the analysis.

2.1.2. Prediction of miR-126 target genes

The bioinformatics analysis software "TargetScan" was used to predict the possible target genes and binding sites of miR-126, evaluate the probability of miR-126 binding to the potential targets based on the number of binding sites and binding strength, and then screen to obtain the target genes with a higher probability.

2.1.3. Dual-luciferase reporter assay

2.1.3.1. Cell transfection. Human umbilical vein endothelial cells (HUVECs) were used in this experiment and were acquired from Shanghai Zhongqiao Xinzhou Biotechnology Co. vascular endothelial growth factor (VEGF)-3′ untranslated region (UTR)- wild type (WT), VEGF-3′ UTR-mutant (Mut), miR-126-5p mimic and mimic-NC were obtained from ROCHE (China). Preparation and use of cell culture medium: the desired plasmids miR-126 mimic, NC mimics and X-tremegene HP (Cat.6366236001, ROCHE) were dissolved at a ratio of "2 μL of X-tremegene HP per 1 μg of plasmid/well transfected", and then the cell transfection reagents were then mixed in 100 μL opti-MEM (Cat.31985-070, Gibco) and left at room temperature for 20 min. When the cell confluence reached approximately 60 %, the medium was replaced with 200 μL of opti-MEM. The effectiveness of the transfection was assessed by RT−qPCR. The transfected cells were subsequently used in several investigations.

2.1.3.2. Luciferase reporter assay. HUVECs were divided into four groups according to the transfection plasmid protocols, namely, the VEGF-3′ UTR-WT/NC mimic cotransfection group, VEGF-3′ UTR-WT/miR-126 mimic cotransfection group, VEGF-3′ UTR-Mut/NC mimic cotransfection group, and VEGF-3′ UTR-Mut/miR-126 mimic cotransfection group. When the cells grew to logarithmic phase, they were washed with phosphate buffer solution (PBS) (Cat. G0002, Servicebio) 2 times, the medium was aspirated, and 300 μL of PLB solution was added to completely lyse the cells. Intracellular firefly luminescence and Renilla luminescence were detected using the Dual-Luciferase® Reporter Assay System Dual-Luciferase Reporter Assay Kit (Cat. E1910, Promega) and a multifunctional enzyme labelling apparatus, following the manufacturer's instructions. Then, the relative luciferase activity was calculated for each group of cells.

2.2. Cellular experiments

2.2.1. Experimental drug

CSEAE: *Caesalpinia sappan* L. (Heilongjiang Medical Materials Co., Ltd, Harbin, Heilongjiang, China) was identified and catalogued

by Professor Wu Xiuhong of Heilongjiang University of Traditional Chinese Medicine. *Caesalpinia sappan* L. powder (40 mesh) was immersed in ethanol (75 %) for 4 h at a solvent to solid ratio of 10:1, then the sample was heated to 85 °C and extracted at reflux for 2 h, repeated once and evaporated using a vacuum drying oven to obtain the ethyl acetate extract of *Caesalpinia sappan* L. (Leachate≥ 7.0 %, Water≤ 12.0 %).

CSEAE suspension: Dissolving 5 g of Carboxymethyl Cellulose (CMC) powder in 1 L of distilled water and leaving overnight at 4 °C. Then CSEAE is dissolved in 5 ‰ CMC suspension and mixed thoroughly to prepare a concentrated drug suspension containing 0.115 g/mL CSEAE.

2.2.2. CSEAE-mediated serum

In previous studies, our research team has carried out high performance liquid chromatography experiments on the CSEAE-Mediated serum obtained by the CSEAE-Mediated serum preparation method used in this experiment. It has been confirmed that when SD rats were given CSEAE suspension by isovolumetric lavage at 1.15 g/kg/d, a CSEAE-Mediated serum with a blood concentration of 8.52 ± 0.57 μg/mL can be obtained. Compared with higher concentrations of serum, this concentration has similar efficacy in the treatment of AS and is more economical. Therefore, our study continues to use this method to obtain CSEAE-Mediated serum in our experiment.

The Experimental Center of Heilongjiang University of Traditional Chinese Medicine (registration number: SYXK-(Hei) 2016-004) provided a total of 10 male Sprague–Dawley (SD) rats, each weighing between 180–220 g, and were housed in a clean-grade animal laboratory with temperatures ranging between 20–24 °C, humidity between 40–60 %, indoor air velocity of 0.1 m/s∼0.2 m/s, 12-h (06:00 a.m. to 06:00 p.m.) light-dark cycle lighting, 24-h free water intake, and twice-weekly bedding change. After one week of acclimatisation feeding, the 10 male SD rats were divided equally into two groups using a random number table (control group and Sappan Extract group), and according to the grouping, the drug was administered to SD rats: the control group was given 5 ‰ CMC suspension by isovolumetric gavage, while the Sappan Extract group was given CSEAE suspension by isovolumetric gavage at 1.15 g/kg/d. Each dosing was performed twice daily (08:00 a.m. and 05:00 p.m.). After 7 consecutive days of administration, the rats were anaesthetised by injecting 20 % urethane into the lateral thigh muscle 1 h after the last dose, and then blood samples were collected from the abdominal aorta (2 mL per rat). The blood samples were left at 4 °C for 2 h and then centrifuged for 15 min (3500 r/min) to obtain serum. The serum was then placed at 56 °C for 30 min and filtered through a 0.22 μm microporous membrane to eliminate bacteria. The prepared CSEAE drug serum was stored at −80 °C and restricted for use within one month.

2.2.3. Experimental cell and group programme

HUVECs were used in this experiment and were maintained in DMEM (Cat. 11965092, Gibco) supplemented with 10 % foetal bovine serum (Cat. 10270-106, Gibco) and 1 % penicillin–streptomycin (Cat. KGY002, Keygen Biotech). The medium used in this experiment includes the following 3 types, Complete medium: DMEM medium, 10 % blank serum, 1 % antibiotics; CSEAE medicated serum medium: DMEM medium, 10 % CSEAE-Mediated serum, 1 % antibiotics; Transfection medium: the complete medium was replaced with a complete medium without antibiotics before cell transfection.

The cells were housed in an incubator with a 5 % CO2 atmosphere at a consistent temperature of 37 °C and were divided into 5 groups: the control group, model group, miR-126 mimic group, Sappan extract group, and combined treatment group. In this experiment, HUVECs were treated with oxidized-low-density lipoprotein cholesterol (Ox-LDL) solution at a concentration of 100 μg/mL for 12 h to induce a model of endothelial cell injury. Our study treated 5 groups of cells simultaneously using different treatment protocols, as shown below. Control group: complete medium incubation for 48 h. Model group: Ox-LDL solution 12 h + complete medium incubation for 36 h miR-126 mimic group: Ox-LDL solution 12 h + miR-126 mimic transfection 24 h + complete medium incubation 12 h. Sappan extract group: Ox-LDL solution 12 h + complete medium incubation for 24 h + 1 μg/mL CSEAE medicated serum treatment for 12 h. Combined treatment group: Ox-LDL solution 12 h + miR-126 mimic transfection 24 h + 1 μg/mL CSEAE medicated serum treatment 12 h.

2.2.4. Cell proliferation assay

HUVECs were inoculated with cells at a density of 3 × 104/mL, with each well of a 96-well plate receiving 100 μL and then incubated at 37 °C in a 5 % CO2 environment. When the cells were well attached to the wall and the cells had grown to approximately 60 % confluence, the wells were treated as in the previous protocol. Cell viability was then evaluated using the CCK-8 kit (Cat. C0038MTS, BEYOTIME) following the manufacturer's instructions. Enzyme markers were used to determine the absorbance at 450 nm to determine the number of viable cells in each group.

2.2.5. Flow cytometry assay

HUVECs were digested using 0.25 % trypsin-EDTA (Cat. J160004, HyClone) for 1 min, centrifuged at 1000 r/min for 5 min, collected into centrifuge tubes, and washed twice with PBS. The Annexin V-FITC/PI Apoptosis Detection Kit (Cat. FAK011.100, Neobioscience) was used following the manufacturer's instructions by first diluting concentrated binding buffer to 1× using deionised water, then resuspending the cells using 500 μL of binding buffer, and then adding the Annexin V-FITC 5 μL and propidium iodide (PI) 10 μL, gently mixing and then incubating for 15 min at room temperature (20–25 °C) using aluminium foil for light protection. Finally the level of apoptosis was detected using flow cytometry (Cat. Canto II, BD).

2.2.6. RT–PCR assay

TriQuick Reagent Total RNA Extraction Reagent (Cat. R1100, Solarbio) was used to extract RNA from the collected cells. A certain

amount of RNA extract was diluted with RNase-Free ddH2O, and the spectrophotometer was zeroed with RNase-Free ddH2O. The diluent was measured by OD260 and OD280. The RNA concentration was calculated according to the following formula: final concentration (ng/μL) = (OD260) × (dilution) × 40. Reverse transcription was performed using the Hifair® II 1st Strand cDNA Synthesis (Cat, 11201ES10, YEASEN) kit according to the instructions (RT reaction solution: 5 × PrimeScript RT Master Mix 4 μL, total RNA 2 μg, RNase-free H2O up to 20 μL). The Hieff® qPCR SYBR Green Master Mix (Cat, 11201ES03, YEASEN) kit was used for PCR amplification experiments according to the instructions to detect the mRNA expression of miR-126 and VEGF in each group of cell samples. The sequences of the target genes were queried using the GenBank database to complete the primer design, and U6 and GAPDH were used as the internal reference genes, as shown in Table 1.

2.3. Animal experimentation

2.3.1. Experimental drug

The CSEAE and CSEAE suspension were prepared in the same way as in the cellular experiments. The CSEAE was dissolved in 5 ‰ CMC suspension and mixed thoroughly to prepare a CSEAE suspension with a CSEAE concentration of 0.161 g/mL, and the dose used in this study was an effective dose validated by a large number of previous studies. Atorvastatin Calcium Tablets (Cat. H20051407, Pfizer Pharmaceutical), specification 10 mg, was crushed using a sterilised tamper until it was in the form of powder and then added to 5 ‰ CMC suspension to formulate an atorvastatin suspension with a concentration of atorvastatin of 0.588 mg/mL.

2.3.2. Experimental animals and group programme

Beijing Viton Lihua Laboratory Animal Technology Co., Ltd. (registration number: SYXK-(Beijing)2016-0006) provided a total of 32 8-week-old male apolipoprotein E-knockout (ApoE−/−) mice (quality certificate: No. 110011211105957943) and 10 8-week-old male C57BL/6J mice (quality certificate: No. 110011211105958078). All mice were SPF grade and weighed between 20–24 g each, and all the mice were kept in an environment similar to that of the SD rats. The experimental protocol was approved by the Shenzhen PKU-HKUST Medical Center Institutional Animal Care and Use Committee (2021-850), and all experimental procedures were strictly implemented in accordance with the Declaration of Helsinki.

First, after one week of acclimatisation feeding, 10C57BL/6J mice were given regular chow for 12 weeks to serve as a control group, and 32 ApoE−/− mice were given high-fat chow for 12 weeks to complete AS model replication. Then, at the end of 12 weeks of feeding, 2 ApoE−/− mice were randomly selected to be anaesthetised, and the thoracic aorta was collected. Then, the aorta was fixed, dehydrated, paraffin-embedded, sectioned, and HE-stained, and finally placed under the microscope to observe the pathological morphology of the aorta to determine whether the model replication was successful. When the AS model was successfully established, the remaining 30 ApoE−/− mice were divided into 3 groups, Model, Atorvastatin, and Sappan Extract, with 10 mice in each group. After grouping, mice in each group were administered by continuous isovolumetric gavage for 4 weeks starting from the 13th week. A dose of 10 mL/kg/d was administered once daily, According to the body surface area conversion formula of human and mouse doses, the equivalent dose given to mice is equivalent to 9.1 times the human dose, and the four groups were administered as follows: Control group: 5 ‰ CMC suspension by gavage, 10 mL/kg/d. Model group: 5 ‰ CMC suspension by gavage, 10 mL/kg/d. Atorvastatin group: Atorvastatin suspension was administered by gavage at 10 mL/kg/d, equivalent to an atorvastatin administration dose of 4 mg/kg/d. Sappan extract group: CSEAE suspension was administered by gavage at 10 mL/kg/d, which is equivalent to the CSEAE administered dose of 3.125 g/kg/d [7]. At the end of the 4-week course of gavage, the mice were fasted and allowed to drink freely for 12 h. Then, the mice were anaesthetised and fixed as described for the cellular experiments. Arterial blood was collected by removing the eyeballs at 0.8–1.2 mL, allowed to stand at room temperature for 1 h, and then centrifuged at 4 °C and 3000 r/min for 10 min. The serum from the top layer of the centrifuged serum was placed in EP tubes by pipette and then stored in a refrigerator at −20 °C for later use. Next, the mice were dissected, the thoracic cavity was exposed, and the thoracic aortic vessels were clipped. A portion of the aorta was quickly placed in a freezing tube, frozen in a liquid nitrogen tank, and then transferred to a −80 °C cryogenic refrigerator for storage. A portion of the aorta was trimmed, flattened, fixed in 4 % paraformaldehyde for more than 24 h, then dehydrated using a dehydrator with sequential gradient alcohol dehydration, paraffin-embedded, and then cut into 6 μm slices of uniform thickness and edges, and then preserved at room temperature to be used for HE staining and Immunohistochemical (IHC) staining.

2.3.3. HE staining

Paraffin sections of thoracic aortas from mice were soaked in xylene (Cat. 10023418, Sinopharm Chemical Reagent) for 20 min for

Table 1
Primer design of target genes in the RT−PCR assay of cellular experiments.

Primer name	Primer sequence	Size
miR-126 F	TCGTACCGTGAGTAATAATGCG	75bp
miR-126 R	GCTGTCAACGATACGCTACGTAA	
U6 F	GCTTCGGCAGCACATATACTAAAAT	102bp
U6 R	CGCTTCACGAATTTGCGTGTCAT	
VEGF F	CCTTGCCTTGCTGCTCTACCTC	116bp
VEGF R	TGCGCTGATAGACATCCATGAACT	
GAPDH F	AGAAGGTGGTGAAGCAGGCGTC	110bp
GAPDH R	AAAGGTGGAGGAGTGGGTGTCG	

deparaffinization. Sections were rinsed using an ethanol gradient and then soaked in distilled water for 5 min to wash away ethanol. Sections were stained using haematoxylin (Cat. G1004, Servicebio) for 5 min, followed by ethanol differentiation using 1 % hydrochloric acid for 2 s, then immediately washed in water to counterstain for 10 min, and then stained in 0.5 % eosin (Cat. G1001, Servicebio) for 2 min. Stained sections were dehydrated using a gradient of ethanol, and then sections were immersed in xylene 2 times for 2 min each to make the specimens transparent. Finally, the sections were sealed using neutral gum (Cat. 10004160, Sinopharm Chemical Reagent) and dried, the pathological morphology of the aorta in each group of mice was observed by light microscopy, and the images were captured and analysed.

2.3.4. Oil red O staining

The fresh frozen tissues of the thoracic aorta of each group of mice were taken. After section fixation, Oil Red O staining, differentiation with 60 % isopropanol, haematoxylin staining, mounting, etc., it was used to observe the lipid content in plaques using a microscope, and the images were captured and analysed.

2.3.5. IHC staining

The paraffin sections were dewaxed and hydrated using xylene and ethanol to expose the antigen. Antigens were repaired using citric acid antigen repair buffer (pH 6.0) (Cat. G1202, Servicebio). Endogenous peroxidase was blocked by immersion using PBS (pH 7.4) (Cat. G0002, Servicebio) solution. A drop of 3 % BSA (Cat. G5001, Servicebio) was added to the histochemistry circle so that the tissue was evenly covered and then placed at room temperature for 30 min for serum closure. The kit instructions were followed for the addition of primary antibody and the addition of secondary antibody, followed by the dropwise addition of the Histochemistry Kit DAB Colour Developer (Cat. G1211, Servicebio) to give a specific brownish yellow colour to CD34-positive tissues of the aorta. Nuclei were restained, differentiated, and redyed using Haematoxylin, Haematoxylin Differentiation Solution (Cat. G1309, Servicebio), and Haematoxylin Reblue Solution (Cat. G1340, Servicebio) to give a blue colour. The specimens were dehydrated, clarified, dried, and sealed, and then the area of CD34-positive staining was observed under a microscope. Images were captured and analysed to determine the microvessel density (MVD) of the aorta and plaque.

2.3.6. RT–PCR assay

Fifty to 100 mg of frozen mouse aortic tissue was ground and homogenised in a mortar and pestle, 1 mL of TriQuick Reagent (Cat, R1100, Solarbio) was added, homogenised until fully lysed, and transferred to a centrifuge tube. The rest of the sections were the same as the corresponding sections in the cell experiments. The primers were designed by searching the sequences of the target genes in the GenBank database, and U6 and GAPDH were used as internal reference genes, as shown in Table 2.

2.3.7. Western blotting assay

Aortic tissue from mice was homogenised with a homogeniser on ice and then centrifuged for 10 min. The supernatant was discarded, 200 μL of RIPA lysate (Cat. BR0002, Best Biological) was added and placed at 4 °C for 30 min to lyse the tissue, and the samples were boiled at 100 °C for 10 min and then placed at 4 °C. Protein quantification was performed using the bicinchoninic acid assay (BCA) assay kit (Cat. P0012, BEYOTIME) following the manufacturer's instructions. The proteins in each sample were separated by 10 % sodium dodecyl sulfate–polyacrylamide gel electrophoresis (SDS–PAGE). Transfer of proteins to a PVDF membrane (Cat. IPVH00010, Millipore) was closed by immersion in a containment solution (Cat. 232100, BD) containing 5 % skim milk powder for 2 h. The blocked membranes were then incubated at 4 °C overnight with primary antibodies, namely, anti-VEGF (diluted 1:1,000, Cat. 19003-1-AP, Proteintech), anti-PI3K (diluted 1:800, Cat. 20584-1-AP, Proteintech), anti-AKT1 (diluted 1:1,0000, Cat. 66444-1-Ig, Proteintech), and GAPDH (diluted 1:3,0000, Cat. HRP-60004, Proteintech). After washing with 1 × TBST (Cat. 21059, Thermo Fisher Scientific), the membranes were incubated with horseradish peroxidase-conjugated secondary antibodies (1:2,000, Cat. 14708S, Cell Signaling Technology) at room temperature for 1.5 h. Target protein bands were visualised using an enhanced chemiluminescence (ECL) kit (Cat. S17851, Yeasen Biotech). An imaging analysis system (Cat. 3200-97001, Clinx) was used to quantitatively examine the protein bands and determine the absorbance value at 562 nm.

2.3.8. ELISA

Mouse serum samples were taken for ELISA. A Mouse Vascular Endothelial Growth Factor Receptor (VEGFR2) ELISA Kit (Cat. JM-12309M1, Jsjingmei) and a Mouse Hypoxia Inducible Factor-1 (HIF-1) ELISA Kit (Cat. JM-02676M1, Jsjingmei) were used according

Table 2
Primer design of target genes in the RT–PCR assay of animal experiments.

Primer name	Primer sequence	Size
miR-126 F	TGCGCTCGTACCGTGAGTAATA	98bp
miR-126 R	CCAGTGCAGGGTCCGAGGTATT	
U6 F	CTCGCTTCGGCAGCACA	103bp
U6 R	AACGCTTCACGAATTTGCGT	
VEGF F	CGATTGAGACCCTGGTGGACA	186bp
VEGF R	GCTGGCTTTGGTGAGGTTTGA	
GAPDH F	ACTCCACTCACGGCAAATTCAA	136bp
GAPDH R	ACATACTCAGCACCGGCCTCAC	

to the manufacturer's instructions for the determination of VEGFR2 and HIF-1 levels in mouse serum.

2.4. Statistical analysis

SPSS 21.0 statistical software was used to analyse the data statistically. Measurement information was expressed as the mean ± standard deviation ($\bar{x} \pm s$), and if it conformed to a normal distribution, one-way ANOVA was used for comparisons between groups, and the LSD method was used for multiple comparisons. Demonstrating the comparison of the proliferation of 5 groups of HUVECs in vitro, the data be analysed by two-way ANOVA to evaluate how the mean of a quantitative variable (OD 450 value) changes according. In this experiment, a p value > 0.05 was considered no statistically significant, a p value < 0.05 was considered statistically significant and p value < 0.01 was considered significant statistical significance for the difference.

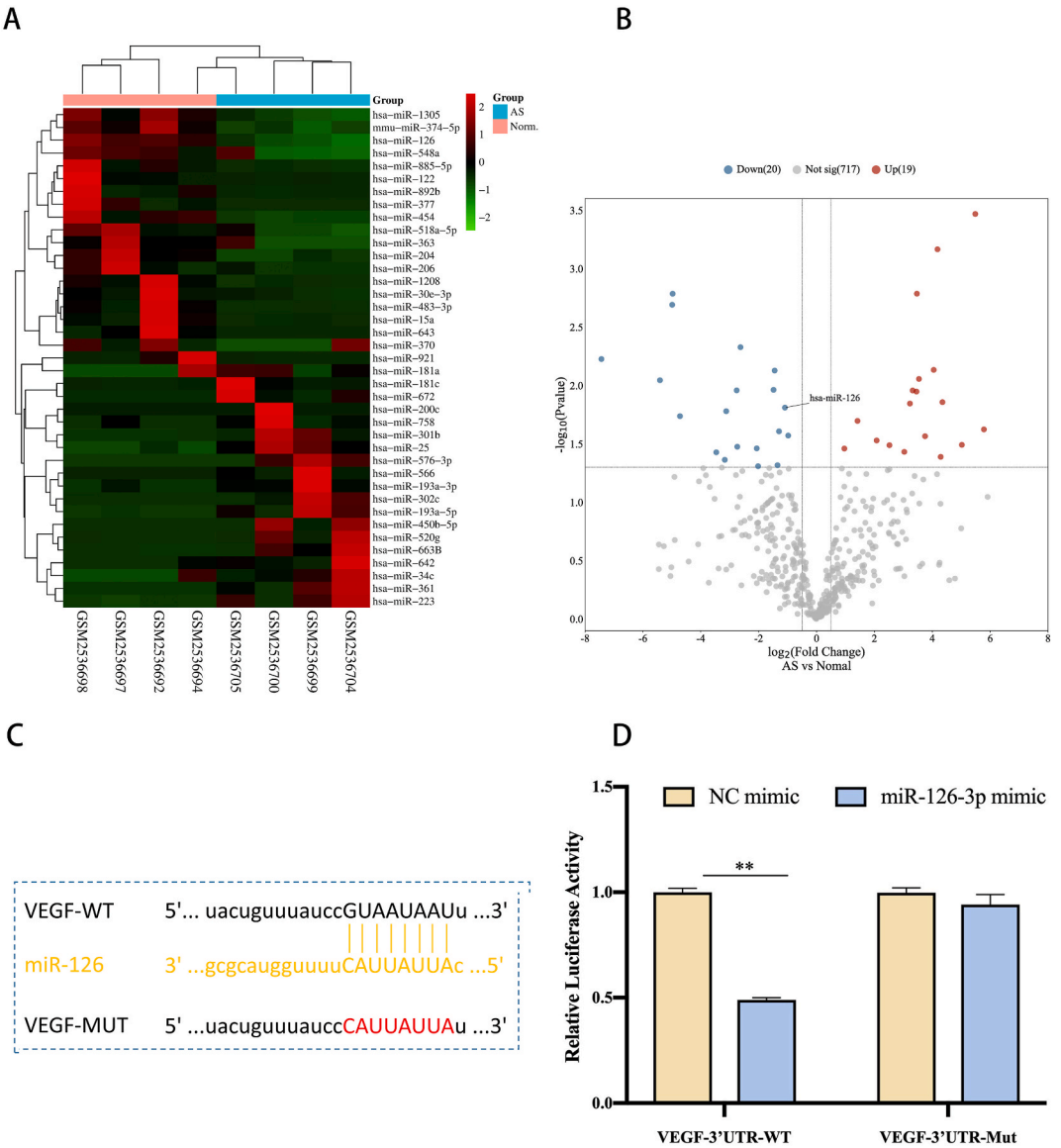

Fig. 1. Target-regulatory relationship between miR-126 and VEGF in HUVECs. (A) Cluster analysis heatmap of differentially expressed miRNAs (Red is high expression, green is low expression, and black is the transition colour). (B) Volcano plot of differentially expressed miRNAs (Red dots are upregulated miRNAs, blue dots are downregulated miRNAs, and grey dots are nonsig miRNAs). (C) Schematic representation of the binding sites between VEGF-3′ UTR-WT or VEGF-3′ UTR-Mut with miR-126-5′ UTR. (D) VEGF-3′ UTR-WT/VEGF-3′ UTR-Mut with miR-126 mimic/NC mimic after cotransfection of luciferase relative activity assay (n = 6). Statistical significance levels: **p value < 0.01.

3. Results

3.1. MiR-126 and VEGF may be potential targets for AS

Differential analysis of the serum whole group miRNA expression matrix from the microarray dataset GSE96621 of 4 AS patients and 4 normal subjects (normal) showed a total of 39 differentially expressed miRNAs in AS (p value < 0.05), which contained 19 miRNAs with upregulated expression (logFC≥ 0.5) and 20 miRNAs with downregulated expression (logFC ≤ -0.5). From this, our study found that there was a significant downregulation of miR-126 expression in the serum of AS patients (p value $= 0.01$, logFC $=$ -1.09) (Fig. 1A–B). TargetScan software prediction results showed a potential binding site between the VEGF-3′ UTR-WT and miR-126-5′ UTR, whereas no possible binding site was found between the VEGF-3′ UTR-Mut and miR-126-5′ UTR (Fig. 1C). The Dual-Luciferase Reporter Assay showed that the expression activity of luciferase was significantly lower in the VEGF-3′ UTR-WT/miR-126 mimic

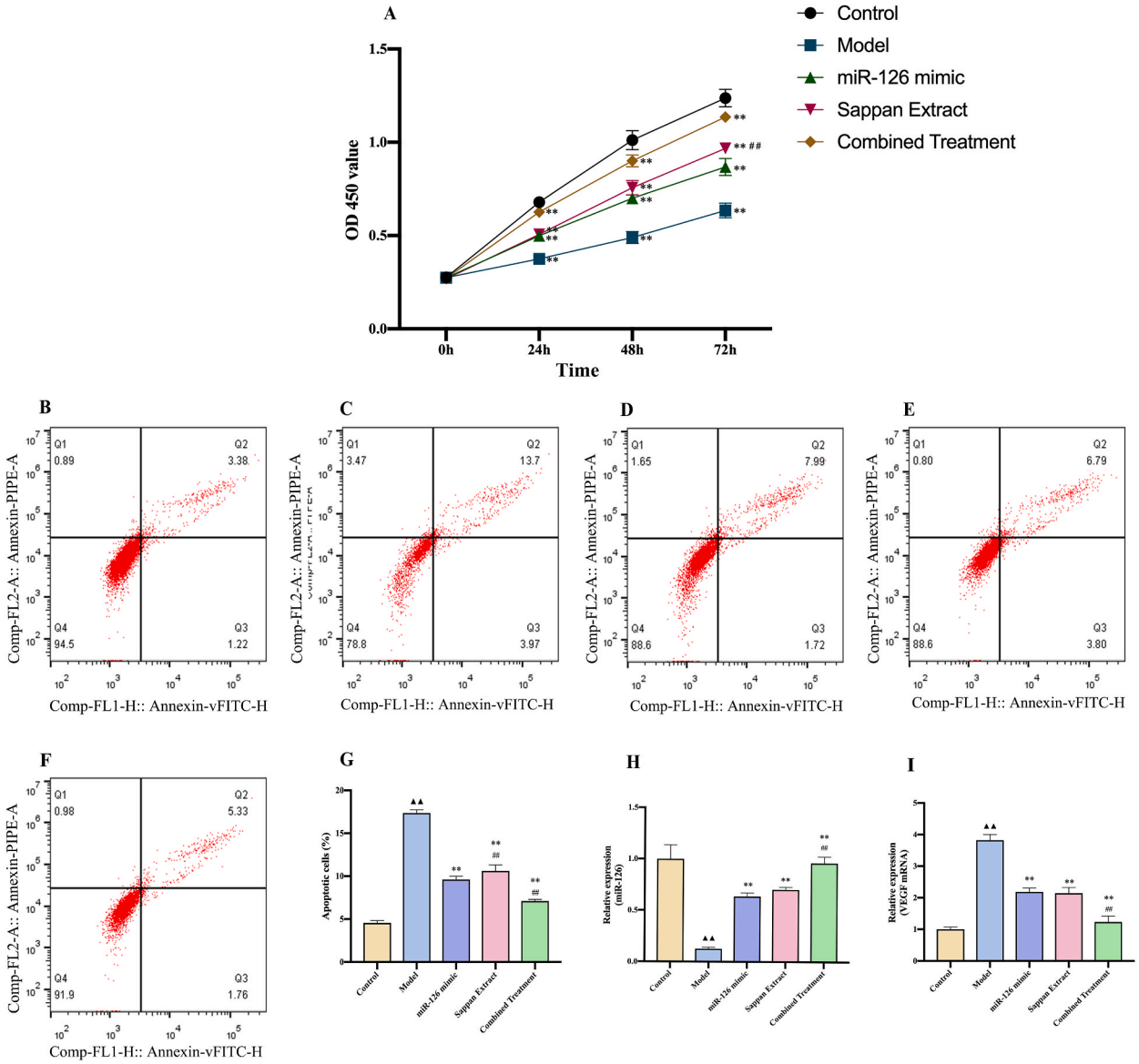

Fig. 2. Effect of CSEAE-Mediated serum on the proliferation and apoptosis levels of HUVECs in vitro (n = 6). (A) Comparison of the proliferation of 5 groups of HUVECs in vitro. (B–G) Levels of apoptosis in vitro in 5 groups of HUVECs. B: Control group, C: Model group, D: miR-126 mimic group, E: Sappan Extract group, F: Combined Treatment group, G: Comparison of apoptosis levels in 5 groups of HUVECs in vitro. (H–I) Effect of CSEAE-Mediated serum on miR-126 and VEGF expression in HUVECs (n = 6). H: Comparison of miR-126 expression in HUVECs, I: Comparison of VEGF mRNA expression in HUVECs. Statistical significance levels: Compared with the Control group, ▲▲p value < 0.01. Compared with the Model group, *p-value<0.05, **p value < 0.01. Compared with the miR-126 mimic group, #p-value<0.05, ##p value < 0.01.

cotransfected group compared to the VEGF-3′ UTR-WT/NC mimic cotransfected group (p value < 0.01); however, there was no statistically significant difference between the VEGF-3′ UTR-Mut/NC mimic cotransfected group and the VEGF-3′ UTR-Mut/miR-126 mimic cotransfected group, suggesting that miR-126 targets and inhibits VEGF expression in HUVECs (Fig. 1D).

3.2. Effect of CSEAE on endothelial cell damage

3.2.1. Effect of CSEAE-mediated serum on proliferation and apoptosis levels of HUVECs in vitro

CCK-8 cell proliferation assay was used to test the proliferation ability of HUVECs in each group at each administration time (Fig. 2A, Table S3), which showed that there was no significant difference in the OD 450 value between the groups at 0 h; after 24–72 h, the proliferation of HUVECs in the miR-126 mimic group, the Sappan Extract group, and the Combined Treatment group was significantly increased compared with that in the Model group (p value < 0.01). In addition, our results also showed that, after 24–48 h, there was no significant difference in OD 450 values between the Sappan Extract groups and miR-126 mimic groups, however, after 72 h, there was a significant difference in OD 450 value between the Sappan Extract group and miR-126 mimic group (p value < 0.05). To evaluate the apoptosis level of HUVECs, our study performed a flow cytometry test on each group (Fig. 2B–F). This result showed that the total apoptosis rate of HUVECs in the Model group was significantly increased compared with that of the Control group; however, the total apoptosis rate of HUVECs in the miR-126 mimic group, Sappan Extract group and Combined Treatment group was significantly decreased compared with that of the Model group. Among them, the total apoptosis rate of HUVECs was significantly

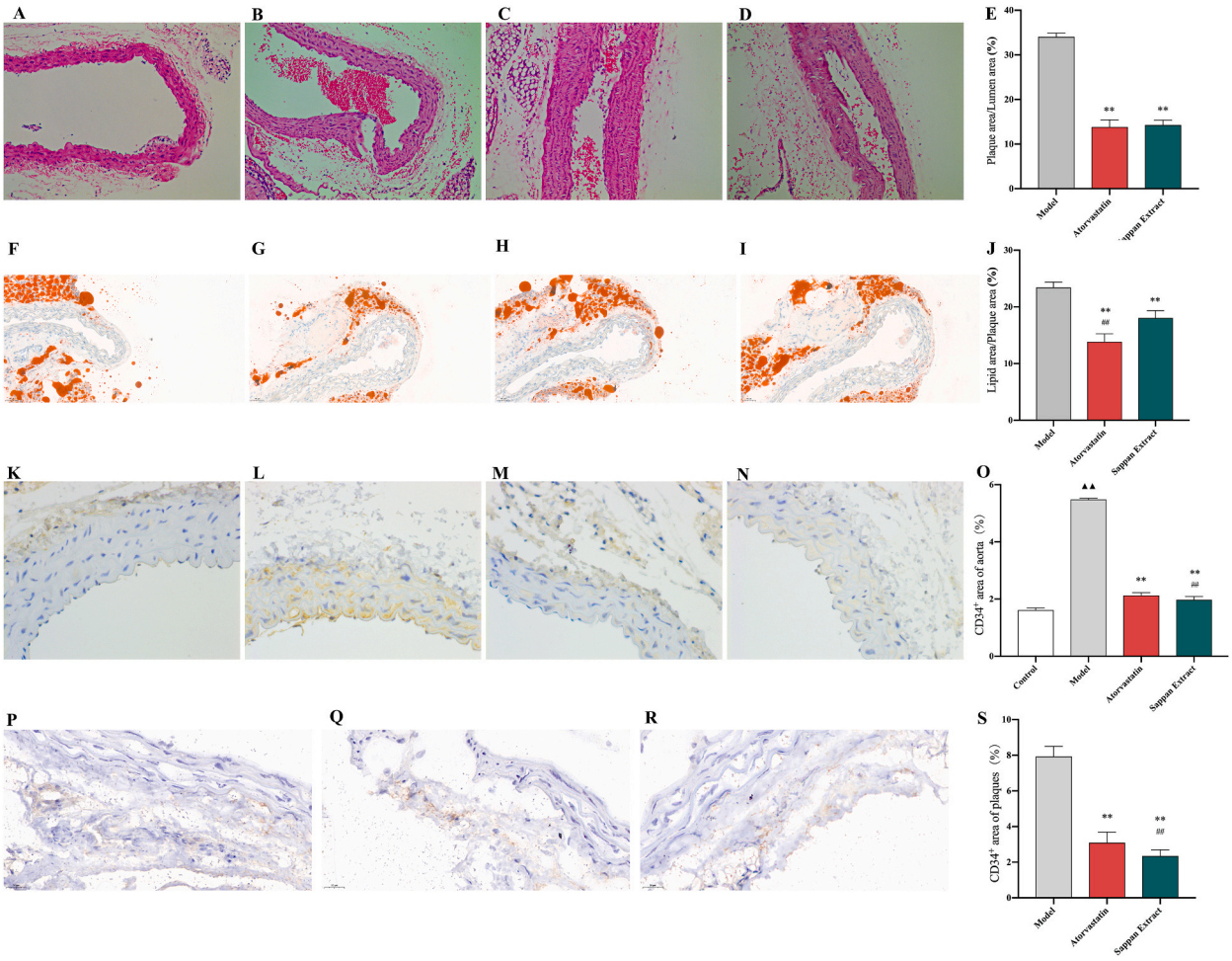

Fig. 3. CSEAE reduces plaque area/lumen area (%) and MVD in AS model ApoE−/− mice (200 ×) (n = 10). (A–E) HE staining of the aortas of mice in each group. A: Control group, B: Model group, C: Atorvastatin group, D: Sappan Extract group, E: comparison of the plaque area/lumen area (%) of the aorta. (F–J) Oil red staining of the aortas of mice in each group, F: Control group, G: Model group, H: Atorvastatin group, I: Sappan Extract group, J: comparison of the lipid area/plaque area (%) of the aorta. (K–O) MVD of the aortas of all 4 groups of mice. K: Control group, L: Model group, M: Atorvastatin group, N: Sappan Extract group, O: Comparison of the MVD of the aorta. (P–T) MVD of ApoE−/− mouse plaques. P: Model group, Q: atorvastatin group, R: Sappan Extract groups, S: Comparison of the MVD of plaques. Statistical significance levels: Compared with the Control group, ▲▲p value < 0.01. Compared with the Model group, **p value < 0.01. Compared with the atorvastatin group, ##p value < 0.01.

lower in the Sappan Extract group and Combined Treatment group than in the miR-126 mimic group (Fig. 2G, Table S4).

3.2.2. Effect of CSEAE-mediated serum on miR-126 and VEGF expression in HUVECs

To determine whether miR-126 expression is downregulated and VEGF expression is upregulated in HUVECs, a model of endothelial injury, and to further clarify whether CSEAE-Mediated serum affects the expression of miR-126 and VEGF mRNA, our study used RT−PCR to evaluate the expression of miR-126 and VEGF mRNA in HUVECs in each group. Compared with that in the control group, the expression level of miR-126 mRNA in HUVECs in the model group was significantly reduced, while the expression level of VEGF mRNA was significantly increased. However, compared with the Model group, the treatments in the miR-126 mimic group, the Sappan Extract group, and the Combined Treatment group significantly promoted the expression of miR-126 mRNA in HUVECs, whereas they significantly inhibited the expression of VEGF mRNA. In addition, our study noted that the effects of the Sappan Extract group were comparable to those of the miR-126 mimic group, while the effects of the Combined Treatment group were significantly better than those of the miR-126 mimic group (Fig. 2H–I, Table S5).

3.3. Effects of CSEAE on AS model ApoE−/− mice

3.3.1. CSEAE reduces plaque area/lumen area (%), lipid area/plaque area (%) and MVD in AS model ApoE−/− mice

First, the HE staining results showed that, the arterial wall of the Control group was clearly layered, the intima thickness was relatively uniform, there was no significant thickening, and no plaque formation was observed, while intima thickening and plaque formation were observed in the aorta of the other 3 groups except the Control group, and the thoracic aorta of model group ApoE−/− mice showed that the aortic wall appeared to be inhomogeneous, noncontinuous, and markedly thickened, the formation of obvious atheromatous plaques could be seen under the endothelium, and the plaque could be seen to be infiltrated by foamy cells with single vacuoles in the cytoplasm or multiple aggregations of tiny vacuoles in a heap. Therefore, our study compared the results of plaque area/lumen area (%) in the Model, Atorvastatin and Sappan Extract groups. Our study found that atorvastatin and CSEAE treatment significantly reduced the plaque area/lumen area (%) of the aorta compared with the model group and were comparable (Fig. 3A–E, Table S6). However, our study further completed the Oil Red O staining experiment, which reveals the formation of plaques inside the blood vessel lumen and the accumulation of foam cells in the intima and media layers, and compared the results of lipid area/plaque area (%) in the Model, Atorvastatin and Sappan Extract groups. Our study found that atorvastatin and CSEAE treatment significantly reduced the lipid area/plaque area (%) of the aorta compared with the model group, and atorvastatin was more effective than CSEAE (Fig. 3F–J, Table S7).

Next, our study examined the area of $CD34^{+}$ staining by IHC staining to determine the MVD of the aorta of all 4 groups of mice (Fig. 3K–O, Table S8), and determined the MVD of the plaques in the Model, Atorvastatin, and Sappan Extract groups (Fig. 3P–S, Table S9). The results of IHC staining showed that the MVD of the intima of the aorta was increased in the Model mice compared to the Control group. Moreover, our study found that both atorvastatin and CSEAE significantly reduced the MVD of the aortic intima and plaques of mice compared with the model group. Notably, CSEAE reduced the MVD of the aortic intima and plaques more significantly

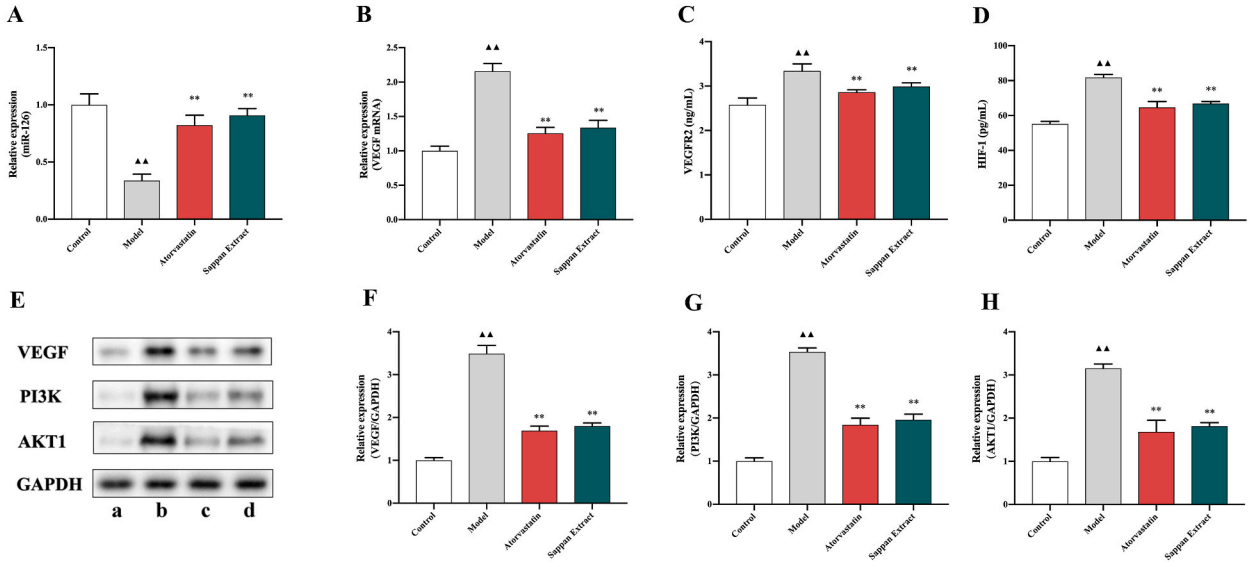

Fig. 4. Effect of CSEAE on the miR-126/VEGF signalling pathway in AS model ApoE−/− mice (n = 10). (A–B) Comparison of miR-126 and VEGF mRNA expression levels in the aortas of mice in each group. A: miR-126. B: VEGF mRNA. (C–D) Comparison of serum levels of VEGFR2 and HIF-1 in various groups of mice. C: VEGFR2. D: HIF-1. (E–H) The protein expression of VEGF, PI3K and AKT1. E: Protein bands (a: Control group, b: Model group, c: Atorvastatin group, d: Sappan Extract group). F: VEGF/GAPDH. G: PI3K/GAPDH. H: AKT1/GAPDH. Statistical significance levels: Compared with the Control group, ▲▲p value < 0.01. Compared with the Model group, **p value < 0.01.

than atorvastatin.

3.3.2. Effect of CSEAE on the miR-126/VEGF signalling pathway in AS model ApoE−/− mice

The RT−PCR assay results (Fig. 4A–B, Table S10) and Western blotting assay results (Fig. 4E–H, Figs. S1–S4, Table S12) showed that the expression level of miR-126 mRNA in the aorta of mice in the Model group was significantly reduced, while the expression level of VEGF mRNA and VEGF, PI3K, and AKT1 protein was significantly increased compared with that of the Control group. However, compared with the Model group, treatment in the Atorvastatin group and the Sappan Extract group both significantly promoted the expression of miR-126 mRNA in the aorta of mice, and both inhibited the expression of VEGF mRNA and VEGF, PI3K, AKT1 protein at the same time. In addition, our study noted that the effects of CSEAE and atorvastatin were similar. Next, ELISA results showed that (Fig. 4C–D, Table S11), compared with the Model group, both the Sappan Extract group and the Atorvastatin group showed significant inhibitory effects on the serum expression of VEGFR2 and HIF-1 in mice. In addition, our study also noted that the effects of CSEAE and atorvastatin were similar.

4. Discussion

Pathological angiogenesis in AS not only promotes plaque formation, but also leads to vessels' immaturity, with profound structural and functional abnormalities, leads to recurrent intraplaque haemorrhage [21]. Thus, inhibit the process of pathological angiogenesis to stabilize, reverse, or even halt AS progression [22]. Over the past 70 years, VEGF has been found to be the most critical factor involved in the angiogenic process. Under pathological conditions, mainly in response to hypoxia or ischemia, elevated VEGF levels promote vascular damage and the growth of abnormal blood vessels. Hence, targeting VEGF or VEGF-mediated molecular pathways could be an excellent therapeutic strategy for managing AS disorders [23]. Recent studies suggested that the miR-126/VEGF signalling pathway is involved in the regulation of cell proliferation, apoptosis, inhibition of angiogenesis and other responses to influence atherosclerosis [24]. Zhao, D. et al. found that endothelial media thickness values and plaque area were negatively correlated with serum miR-126 levels but positively correlated with VEGF [25]. Angiogenic stimuli such as hypoxia through HIF-1, ischemia, oxidative stress, trauma and inflammation promote VEGF activation. The binding of VEGF to VEGFR2 activates a downstream proangiogenic cascade, activates the PI3K/AKT pathway, which regulates cell proliferation and apoptosis and activates several members of the VEGF family [26], which further cross-activates the process of angiogenesis by different mechanisms, such as the promotion of angiogenesis and increase in vascular permeability, promotion of the synthesis and secretion of adhesion molecules and chemokines, induction of intraplaque haemorrhage, increased platelet activation and aggregation, and thrombosis [27,28].

Caesalpinia sappan L., was an ancient Chinese herb medicine for blood-activating and blood stasis-eliminating in treating AS. Therefore, our study speculate that the blood-activating and blood stasis-eliminating effects may be able to regulate the process of angiogenesis in AS. CSEAE, an effective extract of *Caesalpinia sappan* L., our research team has confirmed its clear anti-atherosclerotic therapeutic effect [7], but its role in regulating the mechanism of angiogenesis in AS is still unclear.

Firstly, our study identified a total of 39 miRNAs that were differentially expressed in the serum of AS patients compared to normal human serum by bioinformatics research methods. Notably, the expression level of miR-126 was significantly downregulated in the serum of AS patients compared to normal human serum; however, miR-126 mimics in HUVECs had a significant effect on the luciferase activity of wild-type VEGF reporter gene vectors. In general, miR-126 is highly expressed in endothelial cells, and VEGF is expressed at low levels, with a negative correlation between the two. Combined with the above evidence, our study further speculate that the miR-126/VEGF signalling pathway may be primarily involved in the regulation of angiogenesis in AS.

Next, our study tried to further investigate the mechanism of the effect of CSEAE on the miR-126/VEGF signalling pathway in AS through in vivo and in vitro models of AS, and attempted to explore the effect of CSEAE on the angiogenesis of AS in an in vivo model. AS is a chronic inflammatory vascular disease that occurs in large and medium-sized arteries under a long-term combination of genetic and environmental factors. It is essentially the result of damage to the blood vessel's own tissue cells (e.g., vascular endothelial cells), and intimal thickening and atherosclerotic plaques leading to luminal narrowing are characteristic pathological manifestations of ankylosing spondylitis. Therefore, in this study, HUVECs and ApoE−/− mice were selected as the study subjects, and AS disease models were constructed in vivo and in vitro, respectively.

In the cellular experiments, HUVECs were treated with Ox-LDL solution to induce a model of endothelial cell injury, and the results showed that the proliferation level of the cells in the model group was significantly reduced and the apoptosis level was significantly increased compared with that of the cells not treated with Ox-LDL solution. Moreover, the results of cellular experiments showed that CSEAE-Mediated serum significantly increased the proliferative viability of HUVECs in the endothelial injury model while decreasing their apoptosis level, upregulated the expression of miR-126 and downregulated the expression of VEGF mRNA in HUVECs in the endothelial injury model. These results suggest that CSEAE-Mediated serum modulates the expression of miR-126 and VEGF mRNA, improves proliferation after 24–72 h of treatment and reduces apoptosis in HUVECs to protect endothelial function.

In the animal experiments, combined with the results of HE staining and oil red staining of the aorta in the model group, suggesting that this experiment successfully replicated the ApoE−/− mice model of AS. Our study found significant thickening of the aortic intima and significant plaque formation in the Model group compared with the Control group, and notably, the MVD of both the aortic intima and plaques was significantly increased. Previous findings [29,30] that immunohistochemical staining of arteries from ApoE−/− mice with $CD34^{+}$ cells to assess MVD in an AS model showed a significant increase in MVD in the aortic intima and plaques [31,32], which confirms that this change in increased MVD is prevalent in AS lesions, such as intimal thickening and plaque formation [33], and that angiogenesis is one of the important pathogenic mechanisms in ankylosing spondylitis, which fits with our above findings. Next, our study found that the expression of miR-126 was downregulated in AS model ApoE−/− mice, while the expression of VEGF mRNA and

protein was significantly elevated, and the expression levels of VEGFR2, HIF-1, PIK3, and AKT1 were also high in AS model ApoE−/− mice. This indicates that the level of angiogenesis increases during the formation of AS and is accompanied by changes in the expression levels of the above factors.

As established studies have confirmed, with intimal thickening, plaque formation, and increased cellular oxygen consumption in AS-involved vessels, increased hypoxia and ischemia in the arterial wall induces the release of the proangiogenic factors VEGFR2 [34,35] and HIF-1 [36], which further promotes angiogenesis in arteries and plaques [37,38]. PI3K and AKT1 are the core factors of the classical signalling pathway, PI3K/AKT1 (map04151). Abhinand CS et al. identified early VEGF-induced phosphorylation events in HUVECs, including phosphorylation signalling of the PI3K/AKT1 module, by time-quantified phosphoproteomic analysis of VEGF-treated HUVECs, validating VEGF as an important extracellular signal for PI3K/AKT1 [39]. Several studies have found that when extracellular signals activate intracellular PI3K, PI3K binds specifically to AKT1 and induces AKT1 translocation to the cell membrane and further activates substrate proteins to activate a cascade of downstream reactions, regulating a series of biological processes [40], such as mediating angiogenesis [41], stimulating cell proliferation [42,43], inhibiting apoptosis and improving cell survival [44,45]. Notably, Luo C,. et al. found that the AKT1 pathway activates NF-κB, upregulates IL-6, and activates STAT-3, which leads to an increase in VEGF secretion [46], whereas a study by Dabravolski SA. et al. confirmed that VEGF also activates the AKT1 pathway, and thus, a feedback loop is formed between VEGF and AKT1 that plays a role in upregulating the expression level of VEGF [47]. Combined with the previous discussion, our study further speculate that there is a complex, bidirectional regulatory role between PI3K/AKT1 and VEGF, which may be an important downstream factor in the miR-126/VEGF signalling pathway to regulate angiogenesis. However, new microvessels formed by angiogenesis in arteries and plaques are characterised by functional insufficiency and structural weakness and are prone to rupture and leakage of vascular contents in the hyperinflammatory milieu of AS. Erythrocyte lysis increases cholesterol deposition within the plaque and promotes inflammatory responses and oxidative stress, which in turn further

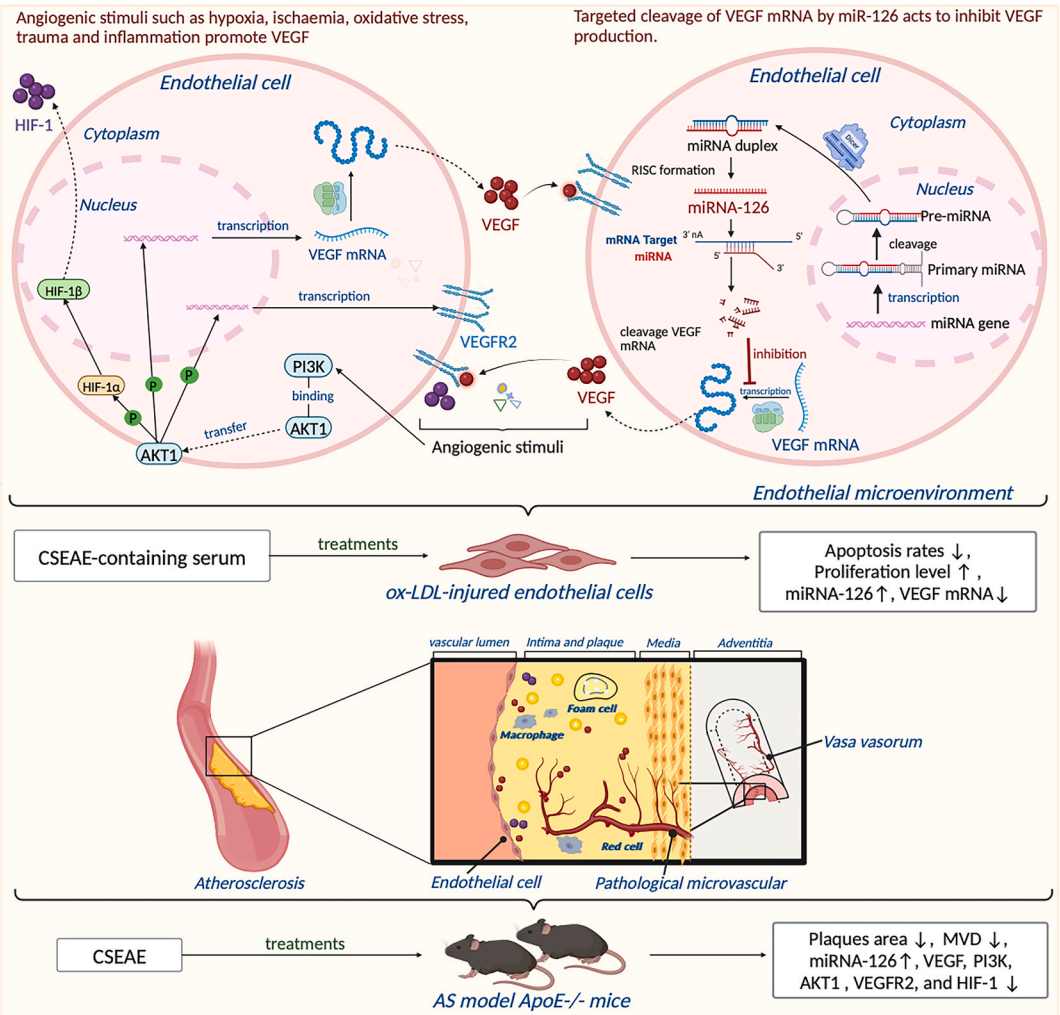

Fig. 5. The mechanism of CSEAE regulated angiogenesis in atherosclerosis by modulating the miR-126/VEGF signalling pathway (Created with BioRender.com).

promotes plaque development and enlargement, leading to intraplaque haemorrhage. Meanwhile, the "plumbing function" of angiogenesis can accelerate plaque formation and development [48]. This finding is consistent with our experimental results, and our animal experimental results further showed that CSEAE significantly reduced the MVD of the aorta and plaques and decreased the aortic plaque area/lumen area (%) and lipid area/plaque area (%) in AS model ApoE−/− mice. Meanwhile, CSEAE promoted the expression of miR-126, inhibited the expression of VEGF mRNA and protein in AS model ApoE−/− mice, and reduced the expression levels of VEGFR2, HIF-1, PIK3 and AKT1. Therefore, our study speculate that the mechanism of CSEAE treatment of AS may be achieved by regulating the miR-126/VEGF signalling pathway, and its possible mechanism is specifically shown in Fig. 5.

Although our basic study did not use high performance liquid chromatography to identify the specific active ingredients of *Caesalpinia sappan* L. that play a role in angiogenesis, combined with the results of other studies [49], we speculated that *Caesalpinia sappan* L. may not only regulate VEGF, angiogenesis may also be mediated by regulating inflammatory cytokines such as IL-1β, IL-6, p38, and TNF-α in tissue cells.

In conclusion, our study demonstrated that CSEAE has an anti-AS effect that protects endothelial function, reduces plaque formation, and reduces the MVD of the aorta and plaques, and its mechanism may be achieved by regulating the activation of the miR-126/VEGF signalling pathway to inhibit angiogenesis in AS. Due to the limitations of the research conditions, our present study has certain deficiencies, such as the lack of analysis of the specific effects of the main active components of *Caesalpinia sappan* L. extract individual components, and the lack of exploration of the mechanism of interactions between the main components. In addition, the number of target validation in this study is limited, and the above deficiencies will be the further research direction of our research group, with a view to providing more objective basis for the treatment of AS with *Caesalpinia sappan* L. extract.

CRediT authorship contribution statement

Yue He: Writing – original draft, Data curation. **Chao Huang:** Writing – review & editing, Data curation. **Jingjing Chen:** Methodology, Data curation. **Weizeng Shen:** Supervision, Methodology, Data curation.

Ethics statement

The sex of the experimental animals used in our study were all male. The ethics approval number our study received is 2023-844, along with the full name of the ethics committee approving our experiments is SHENZHEN PKU-HKUST Medical Center Experimental Animal Welfare Ethics Committee, and our experiments has been carried out in accordance with either the U.K. Animals (Scientific Procedures) Act, 1986 and associated guidelines, the European Communities Council Directive 2010/63/EU or the National Institutes of Health – Office of Laboratory Animal Welfare policies and laws. All animal studies comply with the ARRIVE guidelines. Our study is consult the American Veterinary Medical Association (AVMA) Guidelines for the Euthanasia of Animals (2020), after administration, the rats and mice were anaesthetised by injecting 20 % urethane into the lateral thigh muscle 1 h after the last dose for anesthesia or euthanasia methods.

Caesalpinia sappan L. (the plants licences be deposited in Heilongjiang Medical Materials Co., Ltd, Harbin, Heilongjiang, China) was identified and catalogued by Professor Wu Xiuhong of Heilongjiang University of Traditional Chinese Medicine.

Data and availability statement

Data will be made available on request. For requesting data, please write to the corresponding author.

Funding

This research was supported by grants from National Natural Science Foundation of China Youth Science Fund Project (81903985), Shenzhen Baoan District Healthcare Basic Research Projects (2023JD256).

Declaration of competing interest

The authors declare that they have no known competing financial interests or personal relationships that could have appeared to influence the work reported in this paper.

Acknowledgments

This work is grateful to the above fundings. In addition, our study also appreciate the Bioinformatics platform for providing support in bioinformatics analysis and plotting, GEO database for providing available data, BioRender.com for providing available illustrations, and Nanshin Surui Biotechnology (Nanjing, China) for providing technical support for this study. This study was performed according to international, national and institutional rules considering animal experiments, clinical studies and biodiversity rights.

Appendix A. Supplementary data

Supplementary data to this article can be found online at https://doi.org/10.1016/j.heliyon.2025.e42159.

References

[1] J. Fan, T. Watanabe, Atherosclerosis: known and unknown, J. Pathol. Int. 72 (3) (2022) 151–160, https://doi.org/10.1111/pin.13202.
[2] P. Libby, The changing landscape of atherosclerosis, J. Nat. 592 (7855) (2021) 524–533, https://doi.org/10.1038/s41586-021-03392-8.
[3] Q. Xue, N. He, Z. Wang, X. Fu, L.H.H. Aung, Y. Liu, M. Li, J.Y. Cho, Y. Yang, T. Yu, Functional roles and mechanisms of ginsenosides from Panax ginseng in atherosclerosis, J. Ginseng Res. 45 (1) (2021) 22–31, https://doi.org/10.1016/j.jgr.2020.07.002.
[4] C. Panchakul, P. Thongdeeying, A. Itharat, W. Pipatrattanaseree, C. Kongkwamcharoen, N.M. Davies, Analytical determination, antioxidant and anti-inflammatory activities of Bhamrung-Lohit a traditional Thai medicine, J. Res. Pharma. Sci. 18 (4) (2023) 449–467, https://doi.org/10.4103/1735-5362.378091.
[5] Y. Jin, Z.W. Tong, H.Y. Gao, Z.H. Wu, Guided isolation of new cytotoxic Cassane diterpenoids from Caesalpinia sappan, J. Chem. Biodivers. 20 (5) (2023) e202300211, https://doi.org/10.1002/cbdv.202300211.
[6] T. Vij, P.P. Anil, R. Shams, K.K. Dash, R. Kalsi, V.K. Pandey, E. Harsányi, B. Kovács, A.M.A. Shaikh, Comprehensive review on bioactive compounds found in Caesalpinia sappan, J. Mol. (Basel, Switzerland) 28 (17) (2023) 6247, https://doi.org/10.3390/molecules28176247.
[7] Z. Liu, H. Wang, C. Li, J. Yang, Q. Suo, Y. Zhou, R. Qie, Ethyl acetate extract of Caesalpinia sappan L. for the treatment of atherosclerosis in ApoE-/- mice and its mechanism, J. Mol. Omics 18 (10) (2022) 977–990, https://doi.org/10.1039/d2mo00254j.
[8] Z. Zhou, Y. Wu, W. Hua, X. Yan, L. Li, A. Zhu, J. Qi, Sappanone A ameliorates acetaminophen-induced acute liver injury in mice, J. Toxicol. 480 (2022) 153336, https://doi.org/10.1016/j.tox.2022.153336.
[9] Z. Wang, Z. Chen, X. Wang, Y. Hu, J. Kong, J. Lai, T. Li, B. Hu, Y. Zhang, X. Zheng, X. Liu, S. Wang, S. Ye, Q. Zhou, C. Zheng, Sappanone a prevents diabetic kidney disease by inhibiting kidney inflammation and fibrosis via the NF-κB signaling pathway, J. Front. Pharmacol. 13 (2022) 953004, https://doi.org/10.3389/fphar.2022.953004.
[10] B.J. Pyun, K. Jo, J.Y. Lee, A. Lee, M.A. Jung, Y.H. Hwang, D.H. Jung, K.Y. Ji, S. Choi, Y.H. Kim, T. Kim, Caesalpinia sappan Linn, Ameliorates allergic nasal inflammation by upregulating the Keap1/Nrf2/HO-1 pathway in an allergic rhinitis mouse model and nasal epithelial cells, J. Antioxidants (Basel, Switzerland) 11 (11) (2022) 2256, https://doi.org/10.3390/antiox11112256.
[11] C. Arjin, S. Hongsibsong, K. Pringproa, M. Seel-Audom, W. Ruksiriwanich, K. Sutan, S.R. Sommano, K. Sringarm, Effect of ethanolic Caesalpinia sappan L. Fraction on in vitro antiviral activity against porcine reproductive and respiratory syndrome virus, J. Vet. Sci. 8 (6) (2021) 106, https://doi.org/10.3390/vetsci8060106.
[12] M. Sasarom, P. Wanachantararak, P. Chaijareenont, S. Okonogi, Antioxidant, antiglycation, and antibacterial of copper oxide nanoparticles synthesized using Caesalpinia Sappan extract, Drug Discov. Ther. 18 (3) (2024) 167–177, https://doi.org/10.5582/ddt.2024.01030.
[13] Y.Z. Wang, Y.L. Wang, H.J. Che, Y.H. Jia, H.F. Wang, L.F. Zuo, K. Yang, T.T. Li, J.X. Wang, A. Sappanone, A natural PDE4 inhibitor with dual anti-inflammatory and antioxidant activities from the heartwood of Caesalpinia sappan L, J. Ethnopharmacol. 304 (2023) 116020, https://doi.org/10.1016/j.jep.2022.116020.
[14] M.R.A. Syamsunarno, R. Safitri, Y. Kamisah, Protective effects of Caesalpinia sappan Linn. and its bioactive compounds on cardiovascular organs, Front. Pharmacol. 12 (2021) 725745, https://doi.org/10.3389/fphar.2021.725745.
[15] Y. Chang, S.K. Huang, W.J. Lu, C.L. Chung, W.L. Chen, S.H. Lu, K.H. Lin, J.R. Sheu, Brazilin isolated from Caesalpinia sappan L. acts as a novel collagen receptor agonist in human platelets, J. Biomed. Sci. 20 (1) (2013) 4, https://doi.org/10.1186/1423-0127-20-4.
[16] Y.J. Wan, L. Xu, W.T. Song, Y.Q. Liu, L.C. Wang, M.B. Zhao, Y. Jiang, L.Y. Liu, K.W. Zeng, P.F. Tu, The ethanolic extract of Caesalpinia sappan heartwood inhibits cerebral ischemia/reperfusion injury in a rat model through a multi-targeted pharmacological mechanism, Front. Pharmacol. 10 (2019) 29, https://doi.org/10.3389/fphar.2019.00029.
[17] F. Wediasari, G.A. Nugroho, Z. Fadhilah, B. Elya, H. Setiawan, T. Mozef, Hypoglycemic effect of a combined Andrographis paniculata and Caesalpinia sappan extract in streptozocin-induced diabetic rats, Adv. Pharmacol. Pharma. Sci. 2020 (2020) 8856129, https://doi.org/10.1155/2020/8856129.
[18] Y. Huang, Y. Qi, J. Du, D. Zhang, Protosappanin A protects against atherosclerosis via anti- hyperlipidemia, anti-inflammation and NF-κB signaling pathway in hyperlipidemic rabbits, Iran. J. Basic Med. Sci. 21 (1) (2018) 33–38, https://doi.org/10.22038/IJBMS.2017.18840.5029.
[19] A.M. Gorabi, M. Ghanbari, T. Sathyapalan, T. Jamialahmadi, A. Sahebkar, Implications of microRNAs in the pathogenesis of atherosclerosis and prospects for therapy, J. Curr. Drug Targets 22 (15) (2021) 1738–1749, https://doi.org/10.2174/1389450122666210120143450.
[20] H.S. Jeong, J.Y. Kim, S.H. Lee, J. Hwang, J.W. Shin, K.S. Song, S. Lee, J. Kim, Synergy of circulating miR-212 with markers for cardiovascular risks to enhance estimation of atherosclerosis presence, PLoS One. 12 (5) (2017) e0177809, https://doi.org/10.1371/journal.pone.0177809.
[21] L. Parma, F. Baganha, P.H.A. Quax, M.R. de Vries, Plaque angiogenesis and intraplaque hemorrhage in atherosclerosis, Eur. J. Pharmacol. 816 (2017) 107–115, https://doi.org/10.1016/j.ejphar.2017.04.028.
[22] A.C. Dudley, A.W. Griffioen, Pathological angiogenesis: mechanisms and therapeutic strategies, J. Angiogenesis 26 (3) (2023) 313–347, https://doi.org/10.1007/s10456-023-09876-7.
[23] A. Ahmad, M.I. Nawaz, Molecular mechanism of VEGF and its role in pathological angiogenesis, J. Cell. Biochem. 123 (12) (2022) 1938–1965, https://doi.org/10.1002/jcb.30344.
[24] Q.Y. Yang, Q. Yu, W.Y. Zeng, M. Zeng, X.L. Zhang, Y.L. Zhang, L. Guo, X.J. Jiang, J.L. Gan, Killing two birds with one stone: miR-126 involvement in both cancer and atherosclerosis, Eur. Rev. Med. Pharmacol. Sci. 26 (17) (2022) 6145–6168, https://doi.org/10.26355/eurrev_202209_29632.
[25] D. Zhao, H. Shao, Effect of blood purification on serum miR-126 and VEGF levels in the process of atherosclerosis in uremic patients under maintenance hemodialysis, Kaohsiung J. Med. Sci. 34 (8) (2018) 447–455, https://doi.org/10.1016/j.kjms.2018.04.004.
[26] S.L. Kastora, J. Eley, M. Gannon, R. Melvin, E. Munro, S.A. Makris, What went wrong with VEGF-A in peripheral arterial disease? A systematic review and biological insights on future therapeutics, J. Vasc. Res. 59 (6) (2022) 381–393, https://doi.org/10.1159/000527079.
[27] Y. Tekabe, M. Kollaros, A. Zerihoun, G. Zhang, M.V. Backer, J.M. Backer, L.L. Johnson, Imaging VEGF receptor expression to identify accelerated atherosclerosis, J. EJNMMI Res. 4 (1) (2014) 41, https://doi.org/10.1186/s13550-014-0041-7.
[28] D. Mihalcea, H. Memis, S. Mihaila, D. Vinereanu, Cardiovascular toxicity induced by vascular endothelial growth factor inhibitors, J. Life (Basel, Switzerland) 13 (2) (2023) 366, https://doi.org/10.3390/life13020366.
[29] P. Nowak-Sliwinska, K. Alitalo, E. Allen, A. Anisimov, A.C. Aplin, R. Auerbach, H.G. Augustin, D.O. Bates, J.R. van Beijnum, R.H.F. Bender, G. Bergers, A. Bikfalvi, J. Bischoff, B.C. Böck, P.C. Brooks, F. Bussolino, B. Cakir, P. Carmeliet, D. Castranova, A.M. Cimpean, A.W. Griffioen, Consensus guidelines for the use and interpretation of angiogenesis assays, J. Angiogenesis 21 (3) (2018) 425–532, https://doi.org/10.1007/s10456-018-9613-x.
[30] T.B. Marvasti, F.J. Alibhai, R.D. Weisel, R.K. Li, CD34+ stem cells: promising roles in cardiac repair and regeneration, Can.J. Cardiol. 35 (10) (2019) 1311–1321, https://doi.org/10.1016/j.cjca.2019.05.037.
[31] D. Kashiwazaki, M. Koh, H. Uchino, N. Akioka, N. Kuwayama, K. Noguchi, S. Kuroda, Hypoxia accelerates intraplaque neovascularization derived from endothelial progenitor cells in carotid stenosis, J. Neurosurg. 131 (3) (2018) 884–891, https://doi.org/10.3171/2018.4.JNS172876.
[32] Y. Fang, R. Yang, Y. Hou, Y. Wang, N. Yang, M. Xu, S. Li, S. Gao, M. Jiang, J. Fan, Y. Hu, Z. Xu, L. Gao, F. Cao, Dual-modality imaging of angiogenesis in unstable atherosclerotic plaques with VEGFR2-targeted upconversion nanoprobes in vivo, J, Mol. Imag. Biol. 24 (5) (2022) 721–731, https://doi.org/10.1007/s11307-022-01721-5.
[33] J.A. Phillippi, On vasa vasorum: a history of advances in understanding the vessels of vessels, Sci. Adv. 8 (16) (2022) eabl6364, https://doi.org/10.1126/sciadv.abl6364.
[34] J.P. Miramontes-González, R. Usategui-Martín, L. Pérez de Isla, R. Alonso, O. Muñiz-Grijalvo, J.L. Díaz-Díaz, D. Zambón, F.F. Jiménez, J. Martín-Vallejo, A. E. Rodríguez Gude, D.L. Jiménez, T. Padro, R. González-Sarmiento, P. Mata, VEGFR2 and OPG genes modify the risk of subclinical coronary atherosclerosis in patients with familial hypercholesterolemia, J. Atherosclerosis 285 (2019) 17–22, https://doi.org/10.1016/j.atherosclerosis.2019.03.019.
[35] L. Wang, H. Ge, L. Peng, B. Wang, A meta-analysis of the relationship between VEGFR2 polymorphisms and atherosclerotic cardiovascular diseases, J. Clin. Cardiol. 42 (10) (2019) 860–865, https://doi.org/10.1002/clc.23233.

[36] X. Li, Q. Zhang, M.I. Nasser, L. Xu, X. Zhang, P. Zhu, Q. He, M. Zhao, Oxygen homeostasis and cardiovascular disease: a role for HIF? J. Biomed. Pharmacother. 128 (2020) 110338 https://doi.org/10.1016/j.biopha.2020.110338.
[37] Y. Xiao, M. Li, T. Ma, H. Ning, L. Liu, AMG232 inhibits angiogenesis in glioma through the p53-RBM4-VEGFR2 pathway, J. Cell Sci. 136 (2) (2023) jcs260270, https://doi.org/10.1242/jcs.260270.
[38] A.K. Knutson, A.L. Williams, W.A. Boisvert, R.V. Shohet, HIF in the heart: development, metabolism, ischemia, and atherosclerosis, J. Clin. Investig. 131 (17) (2021) e137557, https://doi.org/10.1172/JCI137557.
[39] C.S. Abhinand, J. Galipon, M. Mori, P. Ramesh, T.S.K. Prasad, R. Raju, P.R. Sudhakaran, M. Tomita, Temporal phosphoproteomic analysis of VEGF-A signaling in HUVECs: an insight into early signaling events associated with angiogenesis, J. Cell Commun. Signal. 17 (3) (2023) 1067–1079, https://doi.org/10.1007/s12079-023-00736-z.
[40] M.Y. Lee, A.K. Luciano, E. Ackah, J. Rodriguez-Vita, T.A. Bancroft, A. Eichmann, M. Simons, T.R. Kyriakides, M. Morales-Ruiz, W.C. Sessa, Endothelial Akt1 mediates angiogenesis by phosphorylating multiple angiogenic substrates, Proc. Natl. Acad. Sci. U. S. A. 111 (35) (2014) 12865–12870, https://doi.org/10.1073/pnas.1408472111.
[41] J. Tian, L. Cheng, E. Kong, W. Gu, Y. Jiang, Q. Hao, B. Kong, L. Sun, linc00958/miR-185-5p/RSF-1 modulates cisplatin resistance and angiogenesis through AKT1/GSK3β/VEGFA pathway in cervical cancer, Reprod. Biol. Endocrinol.: RB&E 20 (1) (2022) 132, https://doi.org/10.1186/s12958-022-00995-2.
[42] C.C. Dibble, L.C. Cantley, Regulation of mTORC1 by PI3K signaling, Trends Cell Biol. 25 (9) (2015) 545–555, https://doi.org/10.1016/j.tcb.2015.06.002.
[43] X. Duan, D.M. Norris, S.J. Humphrey, P. Yang, K.C. Cooke, W.P. Bultitude, B.L. Parker, O.J. Conway, J.G. Burchfield, J.R. Krycer, F.M. Brodsky, D.E. James, D. J. Fazakerley, Trafficking regulator of GLUT4-1 (TRARG1) is a GSK3 substrate, Biochem. J. 479 (11) (2022) 1237–1256, https://doi.org/10.1042/BCJ20220153.
[44] P. Abeyrathna, Y. Su, The critical role of Akt in cardiovascular function, Vasc. Pharmacol. 74 (2015) 38–48, https://doi.org/10.1016/j.vph.2015.05.008.
[45] W. Link, Introduction to FOXO biology, J, Methods Mol. Biol. 1890 (2019) 1–9, https://doi.org/10.1007/978-1-4939-8900-3_1.
[46] C. Luo, Y. Ruan, P. Sun, H. Wang, W. Yang, Y. Gong, D. Wang, The role of transcription factors in coronary artery disease and myocardial infarction, Front. Biosci. (Landmark edition). 27 (12) (2022) 329, https://doi.org/10.31083/j.fbl2712329.
[47] S.A. Dabravolski, V.A. Khotina, A.V. Omelchenko, V.A. Kalmykov, A.N. Orekhov, The role of the VEGF family in atherosclerosis development and its potential as treatment targets, Int. J. Mol. Sci. 23 (2) (2022) 931, https://doi.org/10.3390/ijms23020931.
[48] V. Musil, J. Sach, D. Kachlik, M. Patzelt, J. Stingl, Vasa vasorum: an old term with new problems, Surg. Radiol. Anat., SRA 40 (10) (2018) 1159–1164, https://doi.org/10.1007/s00276-018-2068-3.
[49] V.K. Sugiaman, J. Jeffrey, S. Naliani, N. Pranata, S. Lelyana, W. Widowati, R. Ferdiansyah, D.S. Hadiprasetyo, V. Ayuni, Brazilin cream from Caesalpinia sappan inhibit periodontal disease: in vivo study, PeerJ 12 (2024) e17642, https://doi.org/10.7717/peerj.17642.